

Research on the improvement of mixed titania and Co(Mn) oxide nano-composite coatings

G Yar-Mukhamedova^{1,3}, M Ved², A Karakurkchi², N Sakhnenko² and R Atchibayev¹

¹Physics Department, Al-Farabi Kazakh National University, IETP, 71 Al-Farabi Avenue, Kazakhstan

²Physical Chemistry Department, National Technical University “Kharkiv Polytechnic Institute”, 2 Kyrpychova Street, 61002 Kharkiv, Ukraine

E-mail: gulmira-alma-ata@mail.ru

Abstract. The structure and the properties of the oxide films formed on titanium in the diphosphate based electrolytes by means of plasma electrolytic oxidizing at direct current density of 2–2.5 A·dm⁻² have been studied. Oxide layers of different composition and content of alloying elements were obtained by modification of electrolytes and variation in current density. The interelectrode voltage during PEO, chemical and phase composition, topography and microstructure of the formed layers depend on the electrolyte composition and applied current density. The spark-discharge regime was shown to be reached at inter-electrode voltage 100 to 130 V depending on the composition of electrolyte. The effect of chemical composition and surface morphology formed mixed oxide films on the corrosion resistance and catalytic activity has been discussed.

1. Introduction

Titanium is the most common oxide in heterogeneous catalysis and photo-catalysis for the purification gas and liquid media from toxicant [1,2]. This fact is attributed to the fairly high chemical stability under different operating conditions, no toxicity, and relatively low cost of this material. At the same time it was found that, in most cases, catalyst materials based on mixed two or three component oxide systems exhibit high activity and selectivity not only in heterogeneous red-ox reactions [3–5] but also in photo-catalytic ones [6–8]. Synthesis of nano-composite catalytic disperse systems based on titania is carried out by various methods, including sol-gel processes [6,9,10].

The formation different kind of oxide layers has been achieved by the anodic oxidation and plasma surface treatment in the sparking regime (plasma electrolytic oxidizing PEO) seems to be the very promising since it does not need the sophisticated facilities, allows to form various types of titania and to incorporate different species into the layer by modification of electrochemical parameters and of electrolyte chemistry [11–14].

Titania layers containing manganese oxides obtained by PEO in acetate-borate electrolyte was noted to be catalytic active in CO conversion to CO₂ [15]. Cobalt-containing oxide coatings on titanium are obtained from a silicate electrolyte with cobalt acetate addition [16]. However, the increase in the catalytic activity of above materials in CO oxidation reaction was achieved by additional impregnation followed by annealing. In [17] catalytic materials on titanium and aluminum doped with transition metal oxides (Mn, Fe, Co, Ni) were obtained in one stage by the PEO method,



and also in two stages combining the PEO treatment, followed by impregnation in solutions. The need for additional technological operations was due to the low content of dopants and the uneven distribution of catalytic components in the surface layers.

Our positive experience [18,19] related to the development of electrolytes and single step PEO regimes for nano-composite manganese-containing oxide coatings forming at valve metals from diphosphate bath. This approach was extended to the synthesis of cobalt-containing layers [20]. Nevertheless the study of cobalt and manganese effect on morphology, and, consequently, the catalytic activity and corrosion resistance of mixed oxide systems is topical and new. In this work some results concerning the chemical composition, topography, corrosion resistance and catalytic properties of the oxide layers formed on Ti by plasma electrolytic treatment and alloying by cobalt, manganese and phosphorus has been presented.

2. Materials and experimental procedure

Titanium alloy sheets of composition, wt.%: Ti – 99.2–99.7, and impurities – 0.3–0.8; were subjected to the plasma electrolytic oxidation. The samples' pre-treatment procedure included mechanical cleaning with sandpaper from contaminants, degreasing in a 0.2–0.3 M NaOH, and etching in a mixture of a 0.1–0.3 M HF and 0.3–0.9 M HNO₃, and thorough rinsing with running water. The PEO treatment of the samples was carried out in the diphosphate solution [19,20], with or without the addition of Co and Mn sulfates (table 1). Anodic polarization of samples was carried out from a stabilized current source by a direct current of different densities (table 1) until the sparking regime was achieved. The treatment lasted 30 minutes after attaining the sparking mode to obtain a uniform oxide layer with dopants. The Ti alloy anode was placed into the electrochemical cell (volume 200 ml) the form of the graphite cathode provided the formation of the uniform modified layer on the both sides of the sheet. The temperature of oxidation (293–300 K) was stabilized by water shield. The thickness of the coatings was at least 15–20 μm.

Table 1. The treatment parameters and the code of the studied samples.

Sample code	Electrolyte composition, mol·dm ⁻³	Current density i , A·dm ⁻²	Addition of alloying elements
1	K ₄ P ₂ O ₇ – 0.5	2.0	–
2	K ₄ P ₂ O ₇ – 0.5; CoSO ₄ – 0.1		Co
3	K ₄ P ₂ O ₇ – 0.5; MnSO ₄ – 0.1	2.5	Mn
4			

The surface of the anodized specimens was observed on scanning electron microscope Hitachi S 4200 at magnification up to 10,000 with attached ESEM-50 Philips EDS analyzer. The backscattering electron image and the energy dispersion analysis were done. The X-ray diffraction was done by a Bruker AXS D8 diffractometer, using Cu Kα radiation and Ni filter. The obtained spectra were analyzed using the CPDF PDF – 2/2001 database.

The susceptibility to corrosion was checked in the free aerated 2 M NaOH and Ringer (composition, mol·dm⁻³: NaCl – 0.15, KCl – 0.004, CaCl₂ – 0.004) solutions by comparing the values of open circuit potentials (E_{oc}). The potentials presented in the paper are given relative to the standard hydrogen electrode (SHE). The catalytic properties of the oxide systems were studied in the model reaction oxidation of carbon (II) oxide to CO₂ as in [18,19].

3. Results and discussion

The stages of the titanium alloy oxidizing at direct current of 2 A·dm⁻² in different electrolytes one can see at chronograms of inter-electrode voltage in figure 1. Section I corresponds to a linear change in the inter-electrode voltage U up to 60 V at first 2 min of oxidizing. This section known as pre-spark stage is almost the same for chronograms in all electrolytes and is attributed with formation of phase titania.

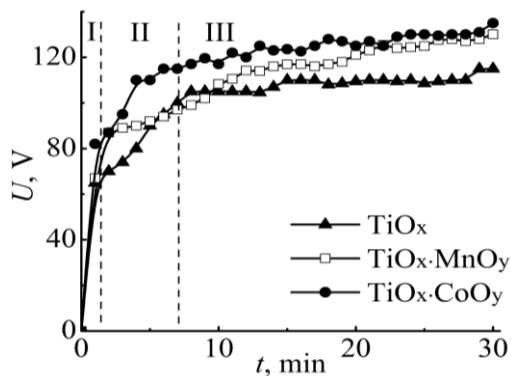


Figure 1. Chronograms of inter-electrode voltage at applied anodic $i=2 \text{ A} \cdot \text{dm}^{-2}$ polarization of Ti alloy in diphosphate electrolyte with or without addition of cobalt or manganese sulfates.

Voltage oscillations are observed in section II of the chronograms, when local sparking begins at the anode. This is due to competitive processes of titania formation / dissolution, and thermo-chemical parallel reactions with electrolyte components. At this stage, the dopants (Co, Mn, P, K) are incorporated into the matrix of titania, forming oxides that heal defects. The dependence of the spark voltage U_s on the nature of the dopants is explained by differences in the specific electrical resistivity of oxides (table 2). It is quite natural that the spark voltage U_s increases in the series $\text{TiO}_2 < \text{TiO}_2 \cdot \text{MnO}_x < \text{TiO}_2 \cdot \text{CoO}_x$.

Table 2. Effect of the current density on the PEO voltage and composition of oxide coatings on Titanium.

Electrolyte	Current density $i, \text{ A} \cdot \text{dm}^{-2}$	Voltage, V		Specific electrical resistance of oxide, $\rho (\Omega \cdot \text{cm})$	Content of dopants in surface layer, P to Ti ratio				
		U_s	U_o		at% Co	Mn	P	K	
$\text{K}_4\text{P}_2\text{O}_7$	2.0	67–73	105	$\text{TiO}_2 - 10^{13}$	–	–	22 ± 1	13.2 ± 0.5	0.53
	2.5		110		–	–	27 ± 1	12.0 ± 0.5	
$\text{K}_4\text{P}_2\text{O}_7, \text{CoSO}_4$	2.0	82–85	120	$\text{CoO} - 10^6 - 10^{10}$	5.7 ± 0.2	–	35 ± 1	10.2 ± 0.5	0.76
	2.5		130	$\text{Co}_3\text{O}_4 - 10^3 - 10^5$	6.3 ± 0.2	–	36 ± 1	7.5 ± 0.5	0.72
	2.0		125	$\text{MnO} - 10^9 - 10^{12}$	–	4.6 ± 0.2	37 ± 1	9.1 ± 0.5	0.63
$\text{K}_4\text{P}_2\text{O}_7, \text{MnSO}_4$	2.5	80–85	130	$\text{Mn}_2\text{O}_3 - 10^5, \text{Mn}_3\text{O}_4 - 10^4 - 10^5$	–	5.0 ± 0.2	38 ± 1	7.6 ± 0.5	0.79
				$\text{MnO}_2 - 10^{-1} - 10^{-3}$	–				

Section III at chronograms corresponds to the micro-arc mode of PEO, and the voltage stabilization is due to the increase in the thickness of the mixed oxide coatings. The operating voltage U_o also depends on the composition of the electrolyte and, consequently, the formed oxides, especially their thermal resistance. The operating voltage in cobalt and manganese containing solutions after 25 min PEO is practically the same, which is due to identical specific electrical resistances MnO and CoO that are the products of intermediate oxides thermal decomposition.

Surface layers morphology depends on the applied current density and composition of oxide coatings. The size of the rounded (doughnut like) grains observed for titanium in diphosphate electrolyte as shown in figure 2(a) increases for Co or Mn containing mixed coatings as shown in figures 2(b) and 2(c) obtained at the same current density $i 2 \text{ A} \cdot \text{dm}^{-2}$, but it decreases at increasing i up to $2.5 \text{ A} \cdot \text{dm}^{-2}$ as shown in figure 2(d). The micro cracks of the doughnut like and of the acicular grains,

have been seen as shown in figure 2(a). The presence of Co ions considerably modified the appearance of the oxide layer as shown in figure 2(b) due to the healing of cracks and defects when dopant is incorporated into the surface layers. On the other hand, the effect of the current density can be seen in the case of layer formation in the Mn containing solution (cf. as shown in figures 2(c) and 2(d)). The structure consisting of the doughnut like grains filled with the small grains has been also observed as shown in figure 2(b). The size of the small grains slightly decreases with the increased i and thus higher Mn content (sample 4).

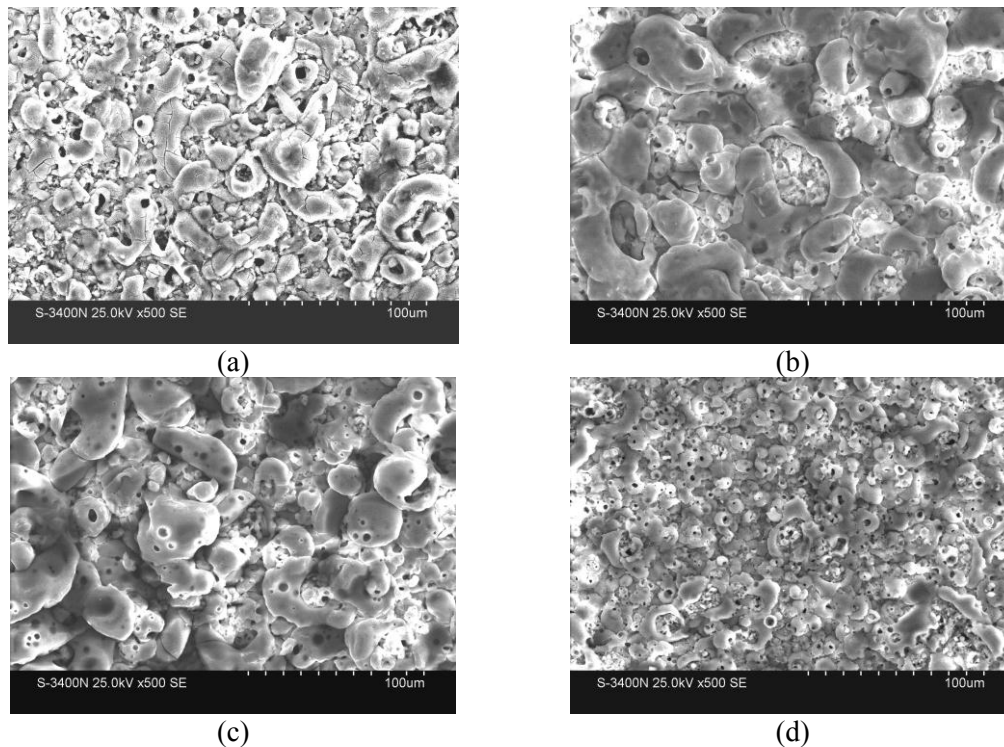


Figure 2. Appearance of the surface of Ti after the PEO treatment at different conditions. Samples: 1 (a), 2 (b), 3 (c), 4 (d).

As follows from the EDS results as shown in figure 3 the X-ray characteristic spectrum taken from the surface reveals the presence of other elements beside Ti and O in the layer. The atomic % of P, K, Co and Mn evaluated from the obtained spectra not taking into account the presence of O, H and B and the ratio of P/Ti are shown in table 2. It is seen that with increasing current and consequent operating voltage the content of Mn, Co and the amount of P and the P/Ti ration increase, whereas the amount of K decreases. The concentration of titanium in the surface valleys of specimen 1 (spectrum 3) is naturally higher than on the peaks (spectrum 2) as shown in figure 3(a). For the other oxide systems this difference is not so noticeable, but at the same time, the content of dopant metals on the peaks (spectrum 2) of the relief is higher than in valleys (spectrum 3) as it follows from figures 3(b) and 3(c).

A series of diffraction lines for α -Ti and TiO_2 on X-ray diffraction patterns for specimens 1, 2, 4 was obtained as shown in figure 4 which is in accordance with [21]. It should be noted that the analysis of the X-ray spectra obtained by the routine procedure shows the presence of the α - P_3Ti_5 in the 1 and 4 specimens. Furthermore, one can find small peaks at angles $2\theta \sim 37^\circ$ and change in intensity double peaks at $2\theta \sim 76^\circ$ on X-ray diffraction patterns of systems $\text{TiO}_x \cdot \text{CoO}_y$ and $\text{TiO}_x \cdot \text{MnO}_y$. Taking into account the data from the EDS, it may be concluded that this difference may be attributed with Co or Mn incorporation in titanium oxide matrix. At the same time the low concentration of these elements does not allow to determine the phase composition with high accuracy.

The results of testing the catalytic activity of the mixed oxide coatings with show that the ignition temperature T_i corresponding to the top efficient operation of a catalyst is in the range from 510 K to 520 K for $\text{TiO}_x\cdot\text{MnO}_y$ systems, obtained by PEO. Parameter T_i is slightly higher than for platinum-based catalysts. The complete conversion of CO at $\text{TiO}_x\cdot\text{MnO}_y$ surface is achieved at $T_c=670$ K (table 3). As can be seen from the data in table 3 mixed oxides $\text{TiO}_x\cdot\text{CoO}_y$ inferior in catalytic activity the $\text{TiO}_x\cdot\text{MnO}_y$ system as it was observed in [18,19]. This is due to variability of manganese oxidation numbers and more developed and a rough surface of mixed manganese containing oxide. Obtained results are in accordance with the data [15–17] and advantage of this work is that observed in this paper coatings do not need additional impregnation. Thus above data confirm the efficiency of materials as catalysts for the CO conversion and gaseous wastes neutralization.

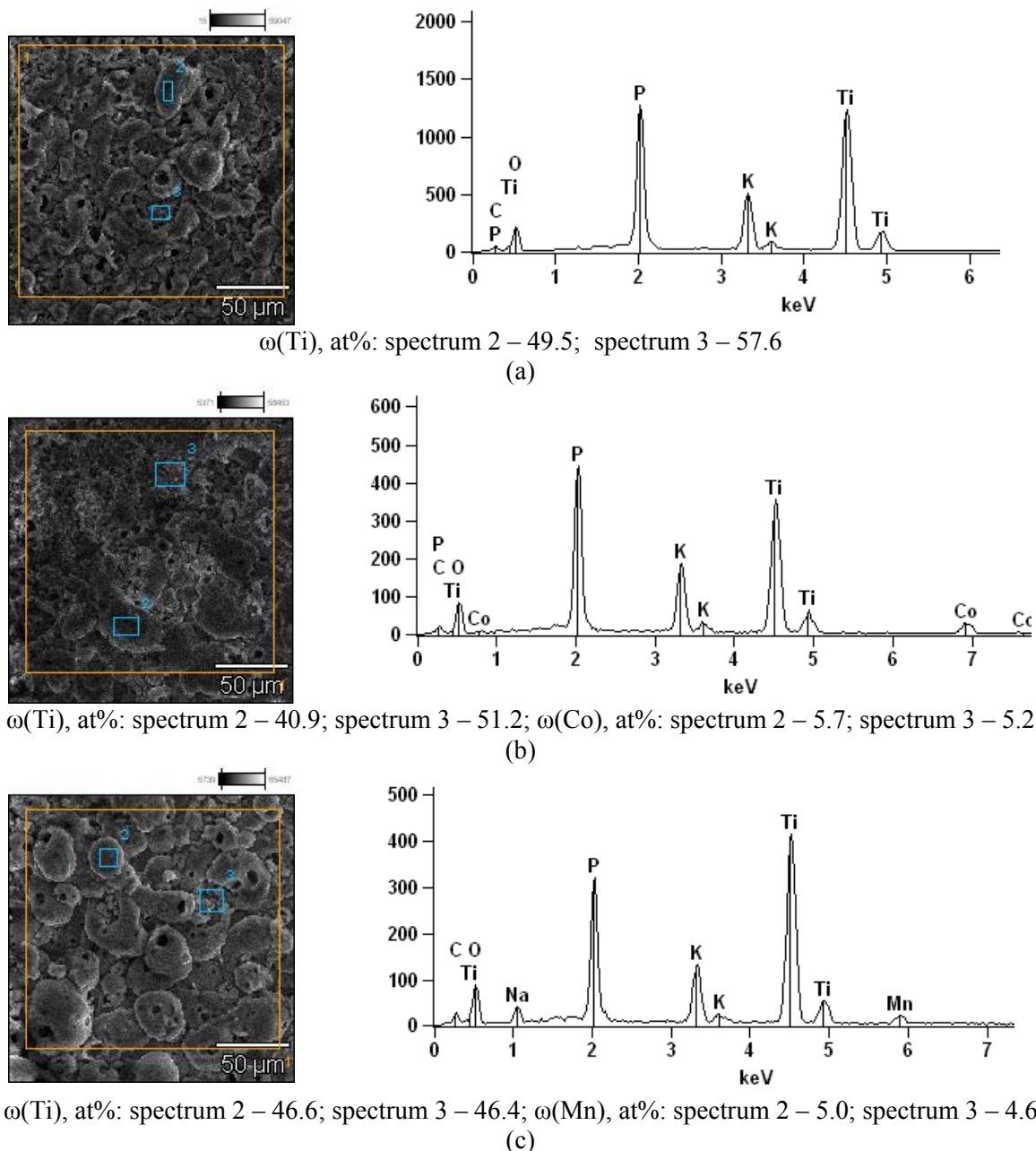


Figure 3. Surface morphology, X-ray spectra taken from the surface and composition of oxide coatings at hills (spectrum 2) ad valleys (spectrum 3) for samples: 1 (a), 2 (b), 4 (c).

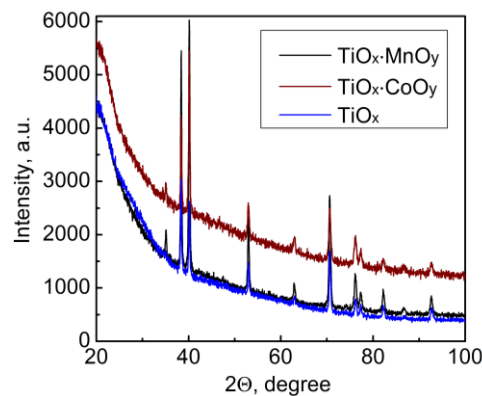


Figure 4. Diffraction patterns of PEO coatings.

Table 3. The catalytic activity of the materials in the CO oxidation reaction.

Catalyst material	The content of the active ingredient ω , at. %	Ignition temperature T_i , K	Temperature of complete conversion T_c , K
Pt [22]	100	490	635
Pt _{exp}	100	495	650
TiO _x ·CoO _y	Co – 6.3	565–570	700–710
TiO _x ·MnO _y	Mn – 5.0	510–520	670–675

Table 4 shows the results of the open circuit potential E_{oc} measurements of samples immersed in 2M NaOH and Ringer solutions. It is seen that PEO substantially increases the corrosion resistance, as follows from the shift of the E_{oc} into the positive direction. The lowest corrosion resistance in both solutions reveals Ti·TiO_x system (sample 1) although it is significantly higher than unoxidized titanium (sample 0).

Table 4. Open circuit potential of oxide systems in different media.

Sample		E_{oc} , mV in solutions	
Code	Composition	2M NaOH	Ringer solutions
0	Ti	–600	–480
1	Ti·TiO _x	370	100
2	TiO _x ·CoO	580	900
4	TiO _x ·MnO _y	450	580

Passivity of doped oxide systems in an alkaline medium is explained by the basic nature of cobalt and manganese oxides. At the same time, it should be noted that manganese oxides are less resistant in chloride-containing media compared to cobalt oxides. Some conclusions may be drawn from the comparison of corrosion behavior data with the surface layers topography. The highest positive open circuit potential of sample 2 may be associated with the closely packed doughnut-like grains filled with small grains, cf. as shown in figure 3(b). The lowest corrosion resistance of sample 1 may be associated with the cracking of the formed layer, which promotes the penetration of electrolyte to the substrate. Specimen 4 has the loosest structure, which may provide lower corrosion resistance as compared with sample 2.

4. Conclusions

- The oxide layers containing the alloying elements might be formed on Ti by means of the anodic polarization in the spark-discharge regime (at current densities 2–2.5 A·dm⁻²).
- The chemical and phase composition as well as the topography, the microstructure of the formed layers can be varied by modification of the electrolytes and by the altering the applied current density.
- The high corrosion resistance of mixed oxide systems in alkaline and in Ringer solutions has been estimated.
- Mixed oxide coatings are characterized by the developed surface and high catalytic activity in the carbon (II) oxide conversion reaction.

References

- [1] Bagheri S, Muhd J N and Bee A H S 2014 *Sci. World J.* **1** 1-21
- [2] Anpo M and Kamat P 2010 *Environmentally Benign Photocatalysts: Applications of Titanium Oxide-based Materials* (Springer Science) pp 234-97
- [3] Rudnev V, Morozova V, Kaidalova T and Nedozerov P 2007 *Russ J Inorg Chem* **52** 1350-4
- [4] Lukiyanchuk I, Rudnev V and Tyrina L 2016 *Surf Coat Technol* **307**(C) 1183-93
- [5] Lukiyanchuk I, Chernykh I, Rudnev V, Ustinov A, Tyrina L, Nedozerov P and Dmitrieva E 2014 *Prot Met Phys Chem Surf* **50** 209-17
- [6] Zaleska A 2008 *Recent Patents on Engineering* **2** 157-64
- [7] Khairy M and Zakaria W 2014 *Egyptian Journal of Petroleum* **23** 419-26
- [8] Sakhnenko N, Ved' M and Bykanova V 2014 *Func mater* **21** 492-7
- [9] Ma X, Zhou W and Chen Y 2017 *Materials* **10** 631
- [10] Yar-Mukhamedova G, Belyaev D, Mussabek G and Sagyndykov A 2017 *SGEM 2017* **17** 107-14
- [11] Gupta P, Tenhundfeld G, Daigle E and Ryabkov D 2007 *Surf Coat Tech* **201** 8746-60
- [12] Wu H, Lu X and Long B 2005 *Mater Lett* **59** 370-5
- [13] Yerokhin A, Nie X and Leyland A 1999 *Surf Coat Technol* **122** 73-93
- [14] Parfenov E, Yerokhin A, Nevyantseva R, Gorbatkov M, Liang C and Matthews A 2015 *Surf Coat Tech* **269** 2-22
- [15] Rudnev V, Vasilyeva M, Kondrikov N and Tyrina L 2005 *Appl Surf Sci* **252** 1211-20
- [16] Vasilyeva M, Rudnev V, Ustinov A, Korotenko I, Modin E and Voitenko O 2010 *Appl Surf Sci* **257** 1239-46
- [17] Lukiyanchuk I, Rudnev V, Tyrina L and Chernykh I 2014 *Appl Surf Sci* **315** 481-9
- [18] Sakhnenko N, Ved M, Karakurkchi A and Galak A 2016 *Eastern-European Journal of Enterprise Technologies* **3** 37-43
- [19] Sakhnenko N, Ved' M, Androshchuk D and Korniy S 2016 *Surf Eng Appl Electrochem* **52** 145-51
- [20] Yar-Mukhamedova G, Ved' M, Karakurkchi A and Sakhnenko N 2017 *IOP Conference Series: Mater Sci and Eng* **213**
- [21] Rokosz K, Hryniewicz T, Raaen S, Chapon P and Dudek L 2017 *Surface and Interface Analysis* **49** 303-15
- [22] Snytnikov P, Belyaev V and Sobyenin V 2007 *Kinet Catal+* **48** 93-102